

## Effect of SiO<sub>2</sub> buffer layers on the structure of SrTiO<sub>3</sub> films grown on silicon by pulsed laser deposition

P. Tejedor, V. M. Fuenzalida, and F. Briones

Citation: *J. Appl. Phys.* **80**, 2799 (1996); doi: 10.1063/1.363198

View online: <http://dx.doi.org/10.1063/1.363198>

View Table of Contents: <http://jap.aip.org/resource/1/JAPIAU/v80/i5>

Published by the [American Institute of Physics](#).

---

### Related Articles

Multiferroic response of nanocrystalline lithium niobate

*J. Appl. Phys.* **111**, 07D907 (2012)

Non-radiative complete surface acoustic wave bandgap for finite-depth hole phononic crystal in lithium niobate

*Appl. Phys. Lett.* **100**, 061912 (2012)

Investigation of dielectric and electrical properties of Mn doped sodium potassium niobate ceramic system using impedance spectroscopy

*J. Appl. Phys.* **110**, 104102 (2011)

Determination of depolarization temperature of (Bi<sub>1/2</sub>Na<sub>1/2</sub>)TiO<sub>3</sub>-based lead-free piezoceramics

*J. Appl. Phys.* **110**, 094108 (2011)

Finite element method simulation of the domain growth kinetics in single-crystal LiTaO<sub>3</sub>: Role of surface conductivity

*J. Appl. Phys.* **110**, 052016 (2011)

---

### Additional information on *J. Appl. Phys.*

Journal Homepage: <http://jap.aip.org/>

Journal Information: [http://jap.aip.org/about/about\\_the\\_journal](http://jap.aip.org/about/about_the_journal)

Top downloads: [http://jap.aip.org/features/most\\_downloaded](http://jap.aip.org/features/most_downloaded)

Information for Authors: <http://jap.aip.org/authors>

## ADVERTISEMENT



Special Topic Section:  
**PHYSICS OF CANCER**

Why cancer? Why physics? [View Articles Now](#)

# Effect of SiO<sub>2</sub> buffer layers on the structure of SrTiO<sub>3</sub> films grown on silicon by pulsed laser deposition

P. Tejedor,<sup>a)</sup> V. M. Fuenzalida,<sup>b)</sup> and F. Briones  
*Centro Nacional de Microelectrónica, C.S.I.C., Serrano 144, 28006 Madrid, Spain*

(Received 19 February 1996; accepted for publication 22 May 1996)

Thin films of SrTiO<sub>3</sub> were grown by pulsed laser deposition on Si and SiO<sub>2</sub>/Si at 35 and 650 °C in a 50 mTorr oxygen discharge (300 V). The effect of introducing a SiO<sub>2</sub> buffer layer between the Si substrate and the complex oxide on the crystallinity and microstructure of the SrTiO<sub>3</sub> films was investigated at both deposition temperatures. All films grown at 35 °C were amorphous. Surface morphology examination by scanning electron microscopy (SEM) showed that these films were continuous and homogeneous when grown on Si, but were porous and had low-density noninterconnecting lines when grown on SiO<sub>2</sub>/Si. Films prepared at 650 °C were polycrystalline and their x-ray-diffraction patterns exhibited peaks corresponding to the (001), (110), (111), and (002) reflections of the SrTiO<sub>3</sub> cubic phase ( $a = 3.904 \text{ \AA}$ ). The films deposited on SiO<sub>2</sub>/Si were found to grow with a high degree of preferred orientation along the (110) direction. SEM studies on the surface morphology of the films grown at high temperature showed the presence of a ‘‘rosette’’ structure. The mean size of the rosettes was  $\sim 80 \text{ nm}$  in 40-nm-thick films grown on Si and  $\sim 100 \text{ nm}$  in films of similar thickness grown on SiO<sub>2</sub>/Si. Additional atomic force microscopy studies on the topography of these samples indicated that the rosettes were constituted by  $\sim 35\text{-nm-diam}$  grains. Typical peak-to-valley surface roughness of these films was 0.5–2 nm. © 1996 American Institute of Physics. [S0021-8979(96)01217-0]

## I. INTRODUCTION

Thin films of high-permittivity dielectric materials have been proposed for applications in high charge storage capacity devices, such as dynamic random access memory (DRAM) capacitors.<sup>1–5</sup> Due to its incipient ferroelectricity (absence of hysteresis loop even at low temperatures) and paraelectric behavior, SrTiO<sub>3</sub> is one of the most promising materials for this type of devices. Its high dielectric constant (300) provides an order of magnitude higher capacitance density than the conventional gate dielectrics, such as SiO<sub>2</sub> and Ta<sub>2</sub>O<sub>5</sub>. Additionally, the lack of fatigue and aging (paraelectricity) problems make this material advantageous with respect to other perovskite ferroelectrics, such as BaTiO<sub>3</sub>, for this particular application. Besides DRAM capacitors, SrTiO<sub>3</sub> has found application as a modifier of the transition temperature of ferroelectric (Ba<sub>x</sub>Sr<sub>1-x</sub>)TiO<sub>3</sub>,<sup>6</sup> as a buffer layer for high-T<sub>c</sub> superconductor thin-film growth on silicon,<sup>7</sup> and as an insulator in superconductor–insulator–superconductor structures.<sup>8</sup> For all these applications, the preparation of SrTiO<sub>3</sub> thin films using silicon as deposition substrate is of special interest to the eventual compatibility of novel complex oxide-based devices with the existing integrated-circuit (IC) technology. One of the major difficulties encountered to date has been the formation of a good interface with reproducible electrical properties between silicon and the complex oxide. Growth on silicon has already been attempted by removing the native SiO<sub>x</sub> layer with a Sr or Ti buffer layer<sup>9,10</sup> and depositing the SrTiO<sub>3</sub> material by electron-beam evaporation. In this way, the native oxide is

reduced to silicon while leaving a Sr or Ti oxide buffer layer. Deposition of SrTiO<sub>3</sub> on silicon by sputtering using metallic Pt/Ti and Pt/Ta double layers as diffusion barriers has also been reported.<sup>11</sup> A different approach, consisting of growing SrTiO<sub>3</sub> thin films by pulsed laser deposition has become a very attractive technique, due to the excellent results achieved to date by a number of research groups.

Although the first report on pulsed laser deposition of SrTiO<sub>3</sub> thin films dates from 1969,<sup>12</sup> it has not been until very recently that this technique has been successfully applied to the preparation of this material for technological purposes. The experimental parameters used in pulsed laser deposition of SrTiO<sub>3</sub> thin films are summarized in Table I. Hitherto, epitaxial films have been grown mainly on SrTiO<sub>3</sub> and MgO substrates with different crystalline orientations, at temperatures between 500 and 760 °C.<sup>8,13–15</sup> MgO substrates were used either bare or covered by Pt or YBaCuO buffer layers. The main effect of the substrate was to change the preferred orientation of the deposited film. Recently, scanning tunneling microscopy (STM) measurements of 1-nm-thick SrTiO<sub>3</sub> films grown on YBaCuO/MgO showed that the microstructure was entirely determined by the substrate, whose defect structure was reflected on the deposited film.<sup>8</sup> Epitaxial growth has also been achieved on MgO-buffered GaAs (100) substrates at 780 °C.<sup>16</sup> Despite its great technological interest, the existing studies on pulsed laser deposition of SrTiO<sub>3</sub> on silicon substrates are rather scarce. Hirano *et al.*<sup>14</sup> reported on the deposition of polycrystalline SrTiO<sub>3</sub> on Si substrates covered by a SiO<sub>2</sub> amorphous layer and observed that optimal crystallinity is achieved at deposition temperatures around 660 °C. These authors observed that the grains were mainly (111) oriented at low deposition temperatures, while the preferred orientations for films grown at temperatures above 660 °C were (110) and (200). Roy and

<sup>a)</sup>Electronic mail: p.tejedor@ic.ac.uk

<sup>b)</sup>On leave from: Universidad de Chile, FCFM, Departamento de Física, Casilla 487-3, Santiago, Chile.

TABLE I. Experimental parameters used in laser-assisted deposition of SrTiO<sub>3</sub>.

Ref.	Substrate	$T$ (°C)	$\lambda$ (nm)	Pulse energy (mJ)	Energy density (J/cm <sup>2</sup> )	Pulse rate (Hz)	$P_{\text{oxygen}}$ (mTorr)	Annealing	Thickness (nm)
6	glass slide	room	1060				$10^{-5}$ <sup>a</sup>	No	
7	MgO(100) Pt/MgO Pt(111)/SiO <sub>2</sub> /Si Pt(111)/glass	650	248	0.6–1.5	0.6–1.5	5	200	46 500 Pa O <sub>2</sub> 60 min 500 °C <i>in situ</i>	350
8	MgO(100) SrTiO <sub>3</sub> (100) YBaCuO(100) SiO <sub>2</sub> /Si	510–760	193	180		10	300		
4	Si Pt/Ti/SiO <sub>2</sub> /Si	400 and 500	248		2		10	400, 500 °C 2 h	300–1000
9	Pt(111)/ MgO(100)	660	193	180		10	30		250–350
10	YBaCuO(100)/ MgO(100)	660	193			4	300	0.2	1
11	MgO(100)/ GaAs(100)	780	308	130	1.3	4	1.2		300–2400
This work	Si(100) SiO <sub>2</sub> /Si(100)	35 and 650	193	100–130	2.5–3	20	50		40–200

<sup>a</sup>Total pressure.

co-workers,<sup>4</sup> on the other hand, obtained fine-grained polycrystalline SrTiO<sub>3</sub> on bare Si and Pt-covered Si substrates at 500 °C, with good electrical characteristics, thus demonstrating the potential use of laser-ablated films for high-density DRAM capacitors.

The aim of this article is to investigate the structural and morphological properties of SrTiO<sub>3</sub> thin films grown on silicon by pulsed laser deposition at different substrate temperatures and to study the effect of introducing a thermally grown stoichiometric SiO<sub>2</sub> buffer layer between the substrate and the complex oxide on the same properties. The interest of using a SiO<sub>2</sub> buffer layer lies in the fact that it can provide a high-quality electrical interface between the semiconductor and the dielectric due to the low density of states present at the SiO<sub>2</sub>/Si boundary, as compared to the ill-defined native SiO<sub>x</sub> layer. After a brief description of the experimental method used to deposit the SrTiO<sub>3</sub> thin films, we present a preliminary characterization of the films by ellipsometry to determine their thickness and refractive index. We then analyze the structural properties of the films by x-ray diffraction (XRD), using both the conventional Bragg diffraction and the grazing-incidence diffraction techniques. Finally, we discuss the film surface morphology on the basis of scanning electron microscopy (SEM) and atomic force microscopy (AFM) data.

## II. EXPERIMENT

Strontium titanate films were deposited using the experimental setup described elsewhere.<sup>17,18</sup> The  $10^{-5}$  Torr deposition chamber was made of stainless steel and was provided with an UV quartz window for laser irradiation. The substrate is placed inside the vacuum chamber at a distance of 30 mm from the target and is heated by means of a tungsten filament. The substrate temperature is measured by a type-K thermocouple placed at the back of the sample. The output of

an ArF excimer laser operating at 193 nm and 20 Hz was focused onto the edge of a 50-mm-diam 7-mm-thick rotating target (20 rpm) of sintered SrTiO<sub>3</sub> to give a typical energy density of 2.5–3.0 J/cm<sup>2</sup>. The substrates were *p*-type Si (100) wafers (10–20  $\Omega$  cm), covered either with a native oxide layer or with a 31.5-nm-thick thermally grown oxide layer. From the standpoint of device application, a very thin (<10 nm), high-capacitance SiO<sub>2</sub> buffer layer is most desirable. Since the emphasis of the present work is on materials properties and thicker layers are easier to grow, a good compromise was found by choosing a nominal thickness of 30 nm. Prior to each experiment the substrates were heated inside the chamber at 200 °C for 0.5 h in 50 mTorr of oxygen. Subsequent deposition of SrTiO<sub>3</sub> was carried out in 50 mTorr of oxygen over a period of 5–20 min to give 30–200-nm-thick films. The deposition temperature was maintained at 650 °C to promote good crystallization. After deposition the samples were quenched to room temperature by turning the heater off, without any further annealing. Some other deposition experiments were performed at 35 °C in order to minimize interface reactions that may be of concern in very thin films.

Film thickness and refractive index were determined by ellipsometry using a PLAS-MOS spot ellipsometer operating at 632.8 nm, with an incidence angle of 70°. Additional thickness measurements were performed on wet-etched (HCl) samples using a Taylor Hobson mechanical stylus. The structural properties (phase and preferred orientation) of the films were studied by conventional Bragg x-ray diffraction (CBD) and grazing-incidence x-ray diffraction (GID) on a Philips PW-1730/10 diffractometer using Cu  $K\alpha$  radiation. The x-ray beam incidence angle in the GID measurements was 1°. Growth morphology (surface and cross section) was examined by means of a Hitachi S-800 field emission SEM. AFM using a Nanoscope III (Digital Instruments) apparatus

TABLE II. Thickness, refractive index, and growth rate of SrTiO<sub>3</sub> films deposited on Si and SiO<sub>2</sub>/Si.

Sample	No. of pulses	Substrate	Temperature (°C)	Thickness (nm)	Refractive index	Growth rate (nm/pulse)	Color
ST-1	7200	Si	35	115±7(105) <sup>a</sup>	1.90±0.02	0.0160	Blue
ST-2	12 000	Si	35	144±4(120)	1.96±0.04	0.0120	Gold
ST-3	7200	Si	35	93±1	1.832±0.003	0.0129	Blue
ST-14	7200	Si	35	74±3	1.74±0.01	0.0103	Violet
ST-5	7200	Si	650	50 (44)	2.246	0.0069	Gold
ST-6	7200	Si	650	39±2	2.25±0.02	0.0054	Gold
ST-7	7200	Si	650	36±2	2.24±0.02	0.0050	Gold
ST-4	7200	SiO <sub>2</sub> /Si	35	75±3(34)	1.84±0.02	0.0104	Blue
ST-13	7200	SiO <sub>2</sub> /Si	35	75±2	1.87±0.02	0.0104	Blue
ST-8	7200	SiO <sub>2</sub> /Si	650	47±1	2.35±0.03	0.0065	Blue
ST-9	7200	SiO <sub>2</sub> /Si	650	43±3	2.31±0.01	0.0060	Blue
ST-11	7200	SiO <sub>2</sub> /Si	650	30±1	2.38±0.02	0.0042	Blue
ST-12	24 000	SiO <sub>2</sub> /Si	650	206±1	2.43±0.03	0.0086	Blue

<sup>a</sup>Data obtained by profilometry.

was used to obtain a more detailed information on the surface topography.

### III. RESULTS AND DISCUSSION

#### A. Thickness and refractive index

Mirrorlike films of SrTiO<sub>3</sub> with thickness comprised between 30 and 200 nm were deposited on Si and SiO<sub>2</sub>/Si at 35 and 650 °C. The thickness, refractive index, and growth rate data are summarized in Table II. In general, we have observed a good agreement between the thickness values obtained by profilometry and by ellipsometry. Given that the latter is a more accurate technique, the ellipsometric measurements were used to estimate the growth rate. As can be seen in Table II, the growth rate for samples grown at room temperature varied between 0.010 and 0.016 nm/pulse, and had lower values, 0.004–0.008 nm/pulse, for samples grown at 650 °C. This difference in growth rates is presumably a consequence of the larger density of the material deposited at high temperature. In Fig. 1 the refractive index is plotted versus the film thickness for SrTiO<sub>3</sub> samples deposited on Si at 35 °C. As can be seen in Fig. 1, the refractive index in-

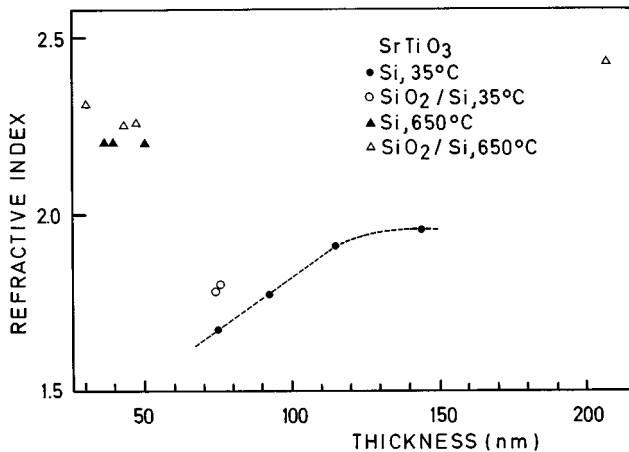


FIG. 1. The refractive index dependence on thickness for SrTiO<sub>3</sub> films deposited on Si at 35 °C.

creases sublinearly with the film thickness and approaches asymptotically the refractive index value of bulk SrTiO<sub>3</sub>. For the other three groups of samples, there are not enough data to derive any dependence of the refractive index on film thickness. It should be noted, however, that the refractive index is clearly larger for films grown at 650 °C, which is consistent with their crystalline microstructure. The crystalline SrTiO<sub>3</sub> material deposited at 650 °C is more refracting than the amorphous one grown at room temperature, as is discussed in the following subsection.

#### B. Crystalline microstructure

XRD techniques have shown that all samples deposited at 35 °C on Si and SiO<sub>2</sub>/Si were amorphous, while those grown at 650 °C were polycrystalline. Figure 2 shows the diffraction patterns obtained by CBD of two samples grown at high temperature on Si and SiO<sub>2</sub>/Si, respectively. In both cases, we observe peaks corresponding to the (001), (110),

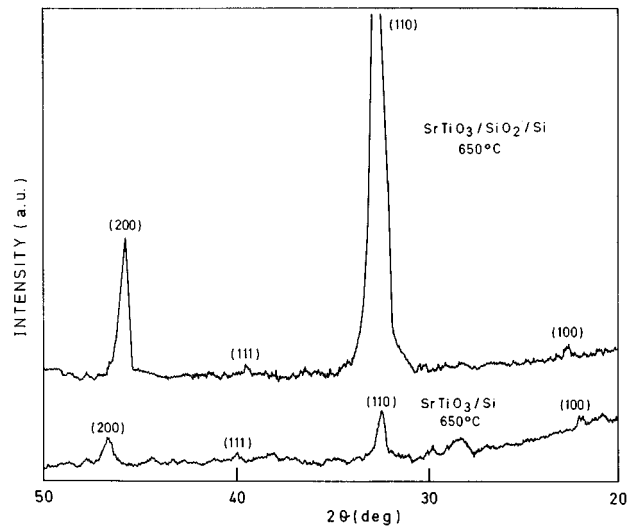


FIG. 2. Conventional Bragg x-ray-diffraction patterns of two SrTiO<sub>3</sub> films grown at 650 °C on (a) SiO<sub>2</sub>/Si and (b) Si. Film thickness: (a) 40 nm and (b) 44 nm.

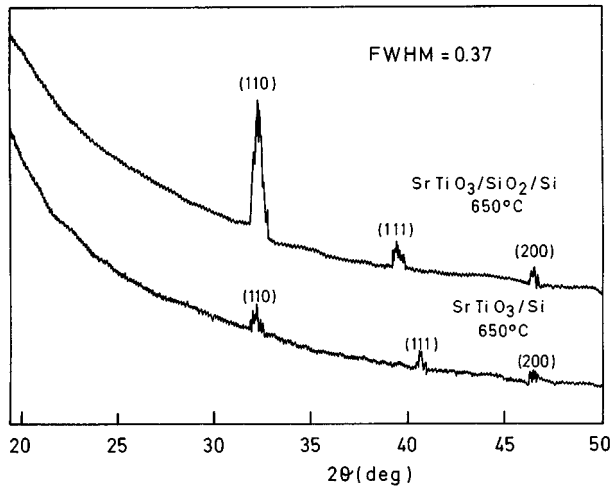


FIG. 3. Grazing-incidence x-ray-diffraction patterns of two SrTiO<sub>3</sub> films grown at 650 °C on (a) SiO<sub>2</sub>/Si and (b) Si. Film thickness: (a) 40 nm and (b) 44 nm.

(111), and (002) reflections of the SrTiO<sub>3</sub> cubic phase. The lattice parameters calculated from the (110) reflection were 3.904 Å for the film grown on Si and 3.906 Å for the film grown on SiO<sub>2</sub>/Si. The intensity ratios of the diffraction peaks are in good agreement with the powder diffraction data. However, considering that both films have similar thickness (~40 nm), the large  $I_{(110)}/I_{(200)}$  ratio (3.7:1) observable in the pattern of the SrTiO<sub>3</sub>/SiO<sub>2</sub>/Si sample with respect to the bulk value (2:1) indicates that the film has a higher degree of texture or preferred orientation in the (110) direction than the SrTiO<sub>3</sub>/Si film. The low diffraction intensities found in the later case, on the other hand, are most probably related to the presence of a thin amorphous layer of native SiO<sub>2</sub> on the Si substrate.

GID was then used to study the in-plane crystallography of the films. Due to the low angle of incidence used in this technique, the x rays are diffracted from lattice planes normal to the surface, thus providing microstructural information in directions parallel to the film–substrate interface. Figure 3 shows the GID radial scan data corresponding to the same samples of Fig. 2. The maximum intensity peak corresponds to the (110) reflection, while the (111) and (002) reflections are almost nonexistent and the (001) reflection is absent in both spectra. The in-plane lattice parameters calculated from the (110) reflection were 3.893 Å, for the sample grown on Si and 3.884 Å for the sample grown on the SiO<sub>2</sub> buffer layer. From the diffraction patterns shown in Fig. 3, we can conclude that, even though certain misalignment with respect to the growth direction may be present in the SrTiO<sub>3</sub>/SiO<sub>2</sub>/Si film, the grains are strongly oriented along the (110) direction, which seems to be the natural orientation of SrTiO<sub>3</sub> films obtained by the pulsed laser deposition technique at the temperature of our experiments, according to Hirano and co-workers.<sup>14</sup> The existence of a preferred orientation in the SrTiO<sub>3</sub>/Si films, nevertheless, is not obvious from the GID data.

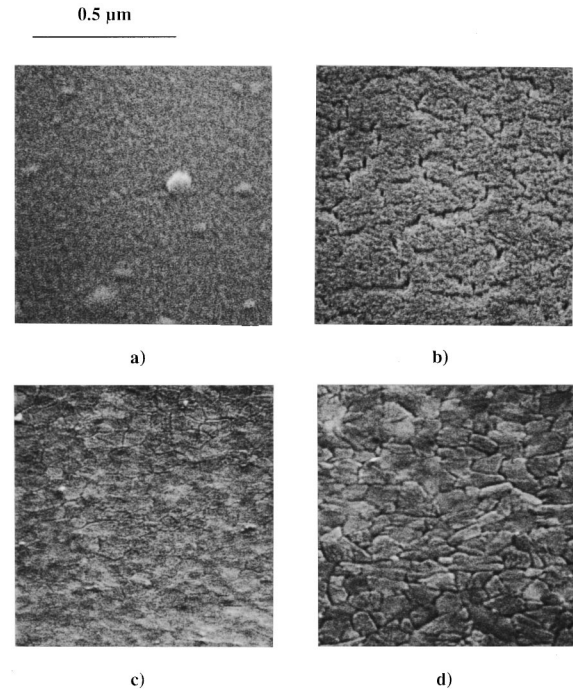


FIG. 4. Scanning electron micrographs showing the surface morphology of four laser-deposited SrTiO<sub>3</sub> films grown at (a) 35 °C on Si, (b) 35 °C on SiO<sub>2</sub>/Si, (c) 650 °C on Si, and (d) 650 °C on SiO<sub>2</sub>/Si. Film thickness: (a) 100 nm; (b) 34 nm; (c) 44 nm; and (d) 40 nm.

### C. Surface morphology

SEM examination of the surface morphology of the samples prepared at 35 °C showed that these films were continuous and homogeneous when grown on Si, whereas those deposited on SiO<sub>2</sub>/Si were porous and exhibited some discontinuities in the form of low-density noninterconnecting lines, as depicted in Figs. 4(a) and 4(b). None of the films obtained at low temperature, whose thicknesses comprised between 35 and 100 nm, showed the presence of defined grains. On the other hand, the films prepared at 650 °C, which were 40–45 nm thick, presented a well-defined columnar grain structure with a mean grain size of ~80 nm for films grown on Si and ~100 nm, for films grown on SiO<sub>2</sub>/Si. The SEM micrographs shown in Figs. 4(c) and 4(d) illustrate the differences in surface morphology exhibited by both samples. It is evident from these micrographs that the grain boundaries are more clearly defined in the film grown on SiO<sub>2</sub>/Si.

The 40-nm-thick SrTiO<sub>3</sub> film grown at 650 °C on SiO<sub>2</sub>/Si shown in Fig. 4(d) was examined by AFM, in order to gain information complementary to SEM regarding its surface topography. Figure 5(a) shows a topographic image of the film surface, where a mosaiclike structure, often called “rosette” structure is observed. The rosettes appeared as grains by SEM and have a mean size of approximately 100–130 nm. They are constituted by a number of grains, which are all similar in diameter (~35 nm) across the film surface. This rosette structure is often seen in complex oxide films and has been well described in the literature by Chapin and Myers.<sup>19,20</sup> A three-dimensional view of the film surface is depicted in Fig. 5(b). As can be observed in Fig. 5(b), the

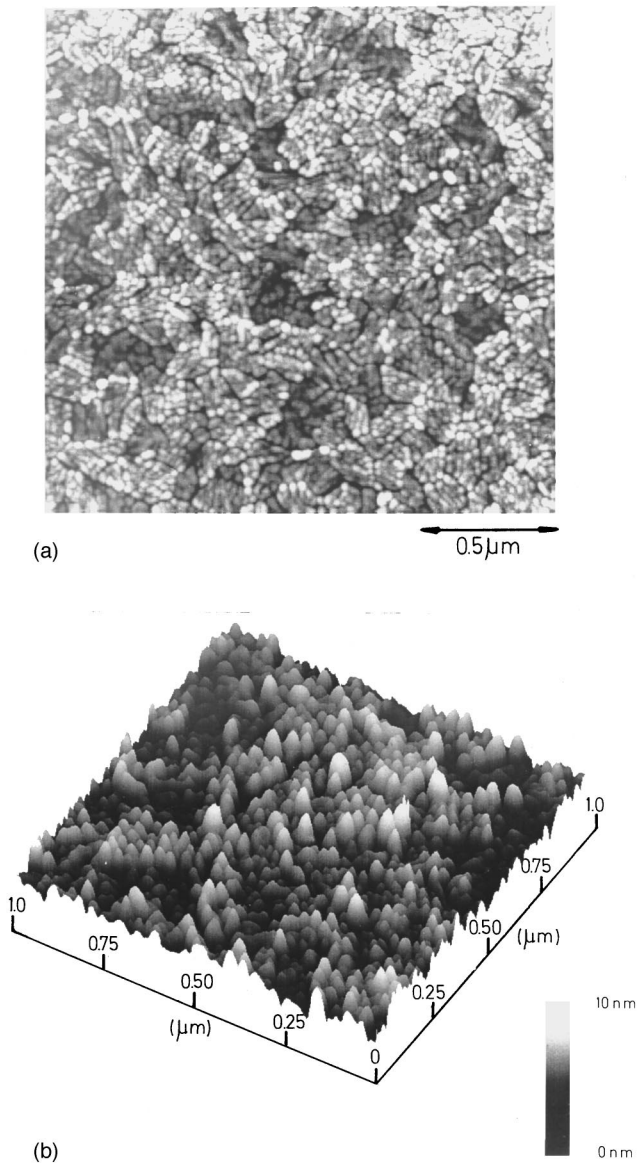


FIG. 5. AFM images showing the surface topography of a 40-nm-thick SrTiO<sub>3</sub> film grown at 650 °C on SiO<sub>2</sub>/Si (a) top view (image size: 2×2 μm<sup>2</sup>), (b) three-dimensional view (image size: 1×1 μm<sup>2</sup>).

rosettes form plateaux arranged in two levels, the upper level being 1.5–2 nm above the lower one. The peak-to-valley surface roughness, measured as the height between a grain boundary and the peak of the grain, was 0.5–2 nm. This result demonstrates that the pulsed laser deposition technique is capable of producing very smooth polycrystalline films of SrTiO<sub>3</sub>.

#### IV. CONCLUSION

We have applied the pulsed laser deposition technique to the preparation of very thin films of SrTiO<sub>3</sub> on silicon substrates at different temperatures and have investigated the effect of introducing a SiO<sub>2</sub> buffer layer on the crystallinity and microstructure of the deposited material. The samples deposited at 35 °C were amorphous, had refraction indexes of 1.74–1.96, and grew at a rate of 0.010–0.016 nm/pulse. None of the films grown at low temperatures had defined

grains; the films deposited on Si were continuous and homogeneous, while those grown on SiO<sub>2</sub>/Si were porous, exhibiting some discontinuities in the form of noninterconnecting lines. The samples deposited at 650 °C, in turn, were polycrystalline and were grown at a rate of 0.004–0.007 nm/pulse. As a consequence of their crystalline nature, these samples were more refringent than those grown at 35 °C, having refractive indexes between 2.24 and 2.43. Although the SrTiO<sub>3</sub> films did not have a single preferred orientation, GID measurements indicated that when a SiO<sub>2</sub> buffer layer was used, the grains showed a strong tendency to grow along the (110) direction. On the other hand, when the SrTiO<sub>3</sub> film was deposited directly on bare Si no clear evidence of preferred orientation was observable in the GID spectra. The films grown at high temperature exhibit a rosette structure appreciable by SEM. The rosettes have a mean size of ~80 nm in films grown on Si and ~100 nm in films grown on SiO<sub>2</sub>/Si. Additional AFM studies on the topography of these samples showed that the “rosettes” formed plateaux arranged in two levels and each of them was constituted by a number of grains. The grains had a mean diameter of ~35 nm for 40-nm-thick films. The typical peak-to-valley surface roughness of the films, as determined by AFM, was 0.5–2 nm, which demonstrates the capability of the pulsed laser deposition technique to provide very smooth films of SrTiO<sub>3</sub>.

#### ACKNOWLEDGMENTS

The authors are pleased to acknowledge R. García and F. J. Tamayo for AFM characterization and J. D. Gómez for SEM micrographs. Ellipsometry measurements were carried out at the Universität der Bundeswehr, Munich. Thanks are due to Professor I. Eisele for many valuable discussions. V.F. would also like to thank the European Community (Contract No. CT91-0875) and Fundación Andes (c-12600-4) for financial support.

- <sup>1</sup> P. C. Joshi and S. B. Krupanidhi, *Appl. Phys. Lett.* **61**, 1525 (1992).
- <sup>2</sup> P. Bhattacharya, T. Komeda, K. Park, and Y. Nishioka, *Jpn. J. Appl. Phys.* **32**, 4103 (1993).
- <sup>3</sup> S. Otani, M. Kimura, and N. Sasaki, *Appl. Phys. Lett.* **63**, 1889 (1993).
- <sup>4</sup> D. Roy, C. J. Peng, and S. B. Krupanidhi, *Appl. Phys. Lett.* **60**, 2478 (1992).
- <sup>5</sup> D. Roy and S. B. Krupanidhi, *Appl. Phys. Lett.* **61**, 2057 (1992).
- <sup>6</sup> V. Mohrotra, S. Kaplan, A. J. Sievers, and E. P. Giannelis, *J. Mater. Res.* **8**, 1209 (1993).
- <sup>7</sup> H. Ishiwaru, N. Tsuki, H. Mori, and H. Nohira, *Appl. Phys. Lett.* **61**, 1459 (1992).
- <sup>8</sup> T. Ohara, K. Sakuta, and T. Kobayashi, *Jpn. J. Appl. Phys.* **32**, 1130 (1993).
- <sup>9</sup> H. Mori and H. Ishiwaru, *Jpn. J. Appl. Phys.* **30**, 1415 (1991).
- <sup>10</sup> B. K. Moon and H. Ishiwaru, *Jpn. J. Appl. Phys.* **33**, 1472 (1994).
- <sup>11</sup> T. Sakuma, S. Yamamichi, S. Matsubara, H. Yamaguchi, and Y. Miyasaka, *Appl. Phys. Lett.* **57**, 2431 (1990).
- <sup>12</sup> H. Schwarz and H. A. Tourtellotte, *J. Vac. Sci. Technol.* **6**, 373 (1969).
- <sup>13</sup> K. F. Etzold, R. A. Roy, and K. I. Saenger, *Mater. Res. Soc. Symp. Proc.* **243**, 489 (1992).
- <sup>14</sup> T. Hirano, T. Fujii, K. Fujino, K. Sakuta, and T. Kobayashi, *Jpn. J. Appl. Phys.* **31**, 511 (1992).
- <sup>15</sup> T. Hirano, M. Taga, and T. Kobayashi, *Jpn. J. Appl. Phys.* **32**, 1760 (1993).
- <sup>16</sup> K. Nashimoto, D. K. Fork, F. A. Ponce, and T. H. Geballe, *Mater. Res. Soc. Symp. Proc.* **243**, 495 (1992).
- <sup>17</sup> P. Tejedor, M. Cagigal, F. Briones, and J. L. Vicent, in *High-*T<sub>c</sub>* Super-*

*conductor Thin Films*, edited by L. Corra (Elsevier, Amsterdam, 1992), p. 541.

<sup>18</sup>P. Tejedor, M. Cagigal, J. L. Vicent, and F. Briones, *Thin Solid Films* **241**, 92 (1994).

<sup>19</sup>L. N. Chapin and S. A. Myers, *Mater. Res. Soc. Symp. Proc.* **200**, 153 (1990).

<sup>20</sup>S. A. Myers and L. N. Chapin, *Mater. Res. Soc. Symp. Proc.* **200**, 231 (1990).